



OPEN

## Optical coherence tomographic angiography study of perfusion recovery after surgical lowering of intraocular pressure

Liang Liu, Hana L. Takusagawa, Miles F. Greenwald, Jie Wang, Brock Alonzo, Beth Edmunds, John C. Morrison, Ou Tan, Yali Jia & David Huang

We investigated the time and location of retinal perfusion recovery after surgical intraocular pressure (IOP) lowering in glaucoma by using optical coherent tomography angiography (OCTA). Seventeen patients were analyzed. The 4.5 × 4.5-mm OCTA scans centered on the disc were performed preoperatively and postoperatively at 6 weeks, 3 months, and 6 months. The peripapillary retinal nerve fiber layer (NFL) thickness, NFL plexus capillary density (NFLP-CD) and visual field (VF) were measured overall and in 8 corresponding sectors. The low-perfusion area (LPA) was used to assess the cumulative area where local NFLP-CD was significantly below normal. At 6 months, the average IOP decreased 5.3 mmHg ( $P = 0.004$ ), LPA decreased by 15% ( $P = 0.005$ ), and NFLP-CD improved by 12% ( $P < 0.001$ ). The NFL thickness and VF mean deviation didn't change significantly at any time point. Among the sectors with significant preoperative NFLP-CD loss, the recovery at 6 months was greatest in sectors with minimal preoperative NFL thinning ( $P < 0.001$ ). In conclusion, surgical IOP lowering may improve NFLP capillary perfusion after 6 months. The perfusion recovery tended to occur in areas with minimal NFL thinning at baseline. OCTA parameters may have potential usefulness as pharmacodynamic biomarkers for glaucoma therapy.

Glaucoma is a leading cause of irreversible blindness in the world and a major source of disability and morbidity in the United States<sup>1,2</sup>. The current treatment of glaucoma has focused on reducing the intraocular pressure (IOP) to slow the progression of the disease. There is evidence that visual field (VF) function could improve after glaucoma surgery, suggesting that some retinal ganglion cells could recover their function if the IOP is sufficiently reduced<sup>3,4</sup>. However, such recovery is difficult to demonstrate by VF due to its poor reproducibility. Very large samples sizes and prolonged follow-up are required to demonstrate statistically significant improvement of VF defects or a decrease in progression<sup>4–12</sup>.

In the last 5 years, optical coherence tomographic angiography (OCTA) has emerged as a noninvasive imaging modality that can complement VF and structural OCT in glaucoma assessment. OCTA parameters such as vessel density and capillary density of the peripapillary retina and the macula have shown high glaucoma diagnostic accuracy and high correlation with VF parameters<sup>13–18</sup>. The measurement of OCTA parameters can be affected by signal strength and other image quality issues, such as shadow or vignetting artifacts, background bulk motion noise<sup>19,20</sup>. OCTA parameters show a diagnostic accuracy of detecting glaucoma comparable with structural OCT parameters in some studies<sup>15–18</sup>, whereas other studies demonstrated structural OCT parameters perform better<sup>21,22</sup>.

Recently, OCTA has been used to investigate responses to glaucoma treatments, with some studies showing improved retinal perfusion following IOP-lowering surgery<sup>23–28</sup>. This is of interest as retinal perfusion could be linked to ganglion cell metabolism and function. Our group has recently developed new methods for assessing focal perfusion changes in the nerve fiber layer plexus (NFLP), the plexus most affected by glaucoma in the peripapillary region<sup>15,29,30</sup>. In this study, we applied these new tools to investigate the extent, location, and timing of perfusion recovery following surgery.

Casey Eye Institute and Department of Ophthalmology, Oregon Health and Science University, 515 SW Campus Drive, Portland, OR 97239-4197, USA. email: [huangd@ohsu.edu](mailto:huangd@ohsu.edu)

Parameter	Preoperative	Postoperative (6 months)	P value
Participant count	17	Same	
Eye count	17	Same	
Age (years)	70 ± 6	Same	
Male/female count	6/11	Same	
Best corrected visual acuity (LogMAR)	-0.02 ± 0.07	0.01 ± 0.08	0.219
Intraocular pressure (mm Hg)	15.9 ± 3.8	10.6 ± 2.7	<b>0.005</b>
Topical ocular antihypertensive, count	2.1 ± 1.1	0.2 ± 0.7	<b>&lt;0.001</b>
Systolic blood pressure (mm Hg)	128.1 ± 13.7	125.8 ± 15.4	0.782
Diastolic blood pressure (mm Hg)	82.8 ± 10.5	82.4 ± 11.2	0.899

**Table 1.** Participant characteristics. *MD* mean deviation, *PSD* pattern standard deviation, *NFL* nerve fiber layer, *NFLP-CD* retina nerve fiber layer plexus capillary density. Group means ± standard deviations are shown unless otherwise noted. The Wilcoxon signed rank test was used. Statistically significant *P* values (<0.05) are in bold type. For the count of topical anti-ocular hypertensives, combination agents are counted as 2 medications.

Parameters	Preoperative	Postoperative–preoperative difference			P value
		6 weeks	3 months	6 months	
IOP (mmHg)	15.9 ± 3.8	-3.7 ± 6.2	<b>-4.7 ± 4.3</b>	-5.3 ± 3.3	<b>0.001</b>
Low perfusion area (mm <sup>2</sup> )	3.91 ± 2.52	-0.18 ± 0.54	-0.003 ± 0.98	<b>-0.57 ± 0.72</b>	<b>0.006</b>
NFLP-CD (% area)	42.7 ± 15.8	2.4 ± 5.0	1.0 ± 6.1	<b>5.3 ± 6.0</b>	<b>0.001</b>
NFL thickness (µm)	67.6 ± 18.8	0.1 ± 3.4	-1.4 ± 4.0	-0.3 ± 4.0	0.486
Rim area (mm <sup>2</sup> )	1.02 ± 0.39	0.02 ± 0.07	0.03 ± 0.07	<b>0.09 ± 0.08</b>	<b>0.002</b>
Cup volume (mm <sup>3</sup> )	0.15 ± 0.17	0.00 ± 0.01	-0.02 ± 0.04	-0.02 ± 0.07	0.157
Cup/disc area ratio	0.43 ± 0.16	0.00 ± 0.05	-0.01 ± 0.05	<b>-0.03 ± 0.04</b>	<b>0.003</b>
VF MD (dB)	-4.61 ± 3.33	N/A	-0.22 ± 1.68	0.02 ± 1.27	0.779
VF PSD (dB)	6.3 ± 3.3	N/A	-0.6 ± 0.8	-0.1 ± 1.1	0.192
VF VFI (%)	88.5 ± 9.5	N/A	0.1 ± 3.3	0.6 ± 2.3	0.651
OCTA images signal strength index	63 ± 5	58 ± 7	61 ± 7	61 ± 6	0.145

**Table 2.** Preoperative values and postoperative changes in outcome parameters. *MD* mean deviation, *PSD* pattern standard deviation, *VFI* visual field index, *NFL* nerve fiber layer, *NFLP-CD* retina nerve fiber layer plexus capillary density, *OCTA* optical coherence tomography angiography. Group means ± standard deviations are shown. *P* values are from the Friedman test to compare the preoperative values and the 3 postoperative values. Statistically significant differences between any one postoperative visit and the preoperative visit ( $P < 0.05/3$ , Wilcoxon test with Bonferroni correction for 3 postoperative visits) are shown in bold type.

## Results

**Study population.** Twenty-two participants were enrolled. One participant was excluded due to postoperative hypotony and 4 participants were excluded due to poor image quality—leaving one eye each of 17 participants for statistical analysis (Table 1). Of these, 11 participants had mild glaucoma and 6 participants had moderate glaucoma according to the modified Hodapp–Parrish–Anderson classification system<sup>31</sup>. All were classified as primary open-angle glaucoma (POAG). All were using at least one ocular antihypertensive medication preoperatively. Trabeculectomy was performed in 15 participants and canaloplasty was performed in 2 participants by different surgeons.

There was no statistically significant difference at preoperative and 6 months postoperative visits for best corrected visual acuity and systolic/diastolic blood pressures (Table 1). As expected, participants had significantly lower IOP and less ocular antihypertensive eye drops use 6 months postoperatively. IOP reduction ranged from 1 to 10 mm Hg.

**Outcome parameters at preoperative and postoperative visits.** After surgery, IOP control significantly improved by 3 months (Table 2). Improvements in perfusion and anatomic parameters lagged—they were only significant at 6 months and not at the earlier visits. Both OCTA perfusion parameters were improved—LPA decreased by 15% and NFLP CD increased by 12%. Some disc anatomic parameters improved—the rim area increased by 8.8% and the cup/disc area ratio decreased by 9.3%. There were no significant correlations ( $P > 0.226$ ) between the perfusion and anatomic improvements and the amount of surgical IOP reduction. There were no statistically significant changes in NFL thickness, VF parameters, or OCTA images signal strength index at any of the postoperative visits (Table 2). The median values and interquartile ranges of OCT and OCTA parameter were showed in Supplementary Table S1.

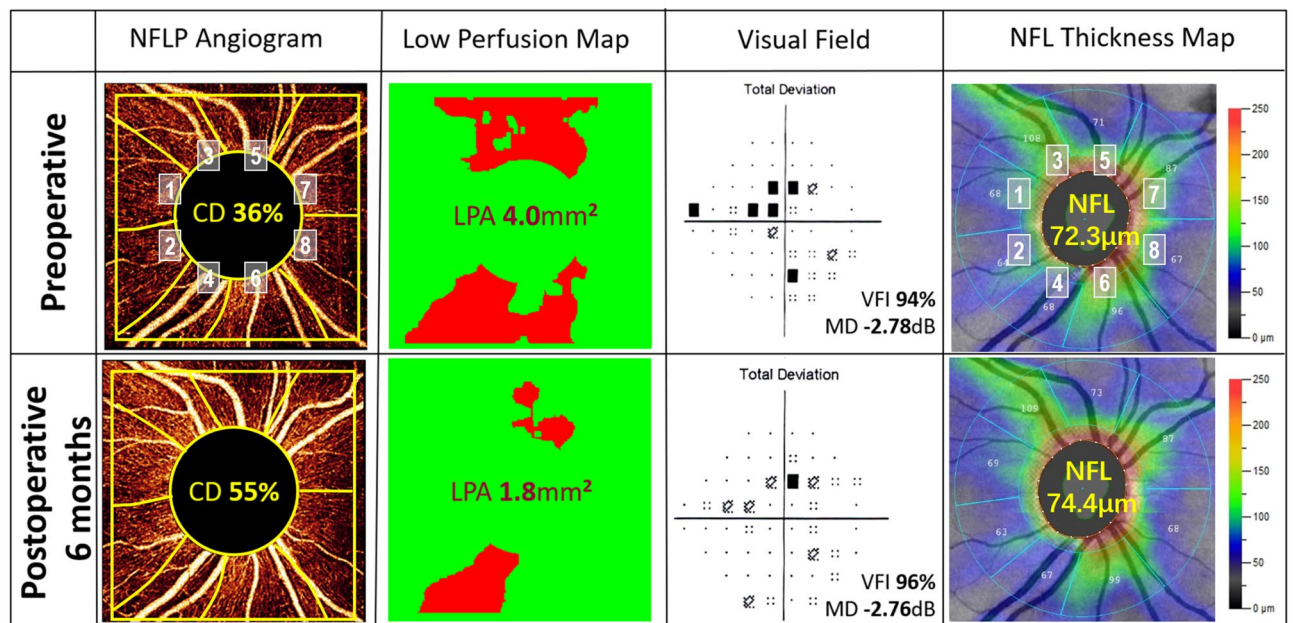


**Figure 1.** A mildly glaucomatous eye showed retinal perfusion recovery at 6 months after trabeculectomy. The nerve fiber layer plexus (NFLP) angiogram was divided into 8 corresponding sectors according to an extended Garway-Heath scheme. This participant had lower IOP (from 16 to 13 mmHg) and less ocular antihypertensive medications use (from 3 to 0) at 6 months postoperatively. The NFLP capillary density (CD) increased by 53%. The low-perfusion map showed the perfusion defects mainly in the sector 3, 4, 5 and 6. The low-perfusion area (LPA) became 55% smaller after surgery. The perfusion recovery occurred primarily in the sector 3 and sector 6, where the NFL thickness were less thinning than the sector 5 and sector 4. The visual field (VF) total deviation map showed shallower defects. The rim area increased from 1.10 to 1.21 mm<sup>2</sup> and the cup/disc area ratio decreased from 0.30 to 0.27. However, the VF mean deviation (MD) and nerve fiber layer (NFL) thickness showed minimal improvement.

**Localization of retinal perfusion improvement.** An eye with mild glaucoma was chosen to demonstrate retinal perfusion recovery 6-month postoperatively (Fig. 1). Wedge-shaped areas of capillary dropout in the superior and inferior hemispheres could be visualized in both the NFLP angiogram and low-perfusion map at the preoperative visit. The low-perfusion map showed the perfusion defects mainly in the sector 3, 4, 5 and 6. Postoperatively, there was more than 50% increase in the average NFLP-CD and reduction in the area of perfusion defect (LPA). The perfusion recovery occurred primarily in the sector 3 and sector 6, where the NFL thickness were less thinning than the sector 5 and sector 4. There were also anatomic and VF improvements, but they were minimal by comparison to the perfusion changes.

**Sectoral analysis of retinal perfusion improvement.** The *en face* OCTA of the NFLP was divided into 8 sectors according to a modified Garway-Heath scheme (Fig. 1). At the baseline visit, the NFLP-CD of all the 136 sectors was 42.4% area (median value, with the interquartile range from 27.9 to 60.7% area). At 6 months, there was a significant sectorwise perfusion recovery ( $P < 0.001$ , Wilcoxon test). The NFLP-CD improved to 53.2% area (median value, with the interquartile range from 32.8 to 63.9% area). Among the 8 modified Garway-Heath sectors in the 17 study eyes, there were 84 sectors (62%) with significant preoperative CD loss (more than 1.96 standard deviation below normal mean). In these 84 sectors, the average improvement of sectoral NFLP-CD at 6 months was 6.7% area ( $P = 0.003$ , linear mixed-effects model, with 95% confidence interval 2.3 to 11.1% area improvement). These sectors were pooled for regression analysis (Fig. 2). In univariate regression analyses (Fig. 2), the sectorwise perfusion recovery, as measured by the 6-month increase in NFLP-CD, was greatest in sectors with minimal preoperative NFL thinning ( $P < 0.001$ ) (Fig. 2A). And the greater perfusion recovery was possible in sectors with moderate preoperative perfusion loss ( $P = 0.029$ ) (Fig. 2B). The multivariate regression analysis yielded the following formula for predicting the postoperative NFLP-CD recovery ( $R^2 = 0.38$ ,  $P < 0.006$ ):

$$\text{NFLP-CD recovery} = 0.635 \times \text{TLB}^2 - 0.801 \times \text{TLB} - 0.577 \times \text{CDLB}^2 + 0.786 \times \text{CDLB} + 0.0306,$$

where TLB is NFL thickness percent loss at baseline, CDLB is NFLP-CD percent loss at baseline.

## Discussions

Our study agrees with 2 previous OCTA studies<sup>24,25</sup> that showed improvement in peripapillary retinal perfusion after IOP-lowering surgery. These 2 studies had significant IOP reductions (18 mmHg and 16 mmHg, respectively) and eyes with more severe glaucoma (VF MD - 13 dB and - 16 dB, respectively), compared to our study. There is also evidence of a similar perfusion improvement after medical reduction of IOP<sup>26</sup>. Four OCTA studies

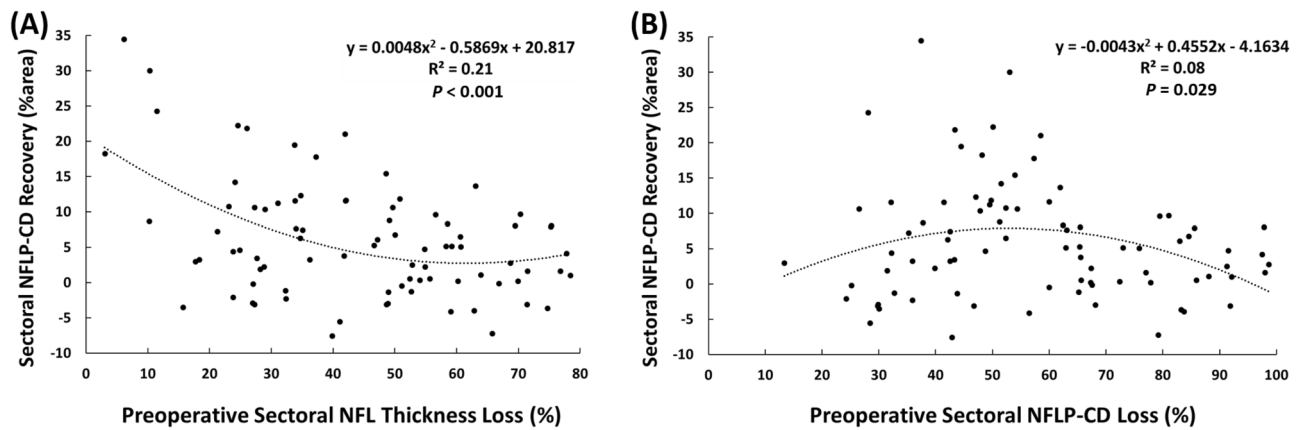


**Figure 2.** The recovery of nerve fiber layer plexus capillary density (NFLP-CD) 6 months after surgery was correlated with preoperative parameters on a sector basis. Sectors with significant preoperative NFLP-CD loss were analyzed. **(A)** The plot against preoperative nerve fiber layer (NFL) thickness loss showed that the perfusion recovery was greatest in sectors with minimal preoperative NFL thinning ( $P < 0.001$ ). **(B)** Plot against preoperative NFLP-CD loss showed greater recovery was possible in sectors with moderate preoperative perfusion loss ( $P = 0.029$ ).

had not found a significant difference in peripapillary retinal perfusion following IOP-lowering surgery<sup>23,27,28,32</sup>. These four studies had relatively small IOP reductions (from 7 to 10 mmHg) and eyes with moderate to severe glaucoma (average VF MD ranged from  $-10$  to  $-15$  dB). One of these study<sup>27</sup> only looked at the 1-month post-operative outcome, which is too soon for perfusion improvement to occur, according to our results. Although the average reduction of IOP was only 5.3 mmHg in our study, we still detected a significant improvement of the peripapillary retinal perfusion. One possible explanation is our study had more mildly glaucomatous eyes with average VF MD  $-4.6$  dB. Since these eyes had less NFL thinning than severe glaucomatous eyes, they might have more perfusion recovery potential.

While the final outcome of this study is the same as previous publications, we were able to analyze the timing and location of perfusion improvements to obtain novel insights. The increase in NFLP-CD and reduction in LPA both occurred gradually after surgery, only becoming significant after 6 months. The perfusion recovery tended to occur in areas with minimal NFL thinning and moderate perfusion loss. These patterns are consistent with the hypothesis that in glaucomatous eyes there exist dysfunctional ganglion cells and nerve fibers that have reduced metabolism and perfusion. These cells have not yet died or lost volume and thickness. They can gradually recover function, metabolism, and perfusion after IOP is reduced to a tolerable level.

Since the perfusion recovery appears to be caused by the IOP reduction, there should be a correlation between the two. However, we did not find a significant correlation between the amount of IOP reduction and the amount of perfusion recovery. This may be due to the modest (mean 5, range 1–10 mm Hg) IOP reduction in our study. In a similar sized trabeculectomy study with a more dramatic IOP reduction (mean 18 mm Hg), In et al. did find that the perfusion recovery was significantly correlated to amount of the IOP reduction<sup>24</sup>.

The existence of injured but viable cells capable of recovery had already been proposed<sup>33</sup> to explain the subset of patients with VF recovery after effective intervention<sup>3,4,34,35</sup>. Longitudinal data from the Collaborative Initial Glaucoma Treatment Study (CIGTS) showed that over 5 years, 14% of patients undergoing IOP-lowering therapy had significant improvement in their VF compared to baseline and that better IOP control was a predictive factor for VF improvement<sup>3</sup>. Caprioli et al. also reported improvement in VF 5 year following trabeculectomy<sup>4</sup>. However, others have found that VF loss did not significantly improve following IOP-lowering<sup>5,6</sup>. These findings can be reconciled if we take into account the high test–retest variability of VF results, which necessitates many tests and large cohorts to yield statistically significant results. The findings in our modest cohort suggest that OCTA may be able to detect post-intervention changes more quickly and easily than VF.

While viable ganglion cells could recover, cells that have undergone apoptosis should not be able to regenerate. Thinning of the NFL is an indication of cell loss, which theoretically would be irreversible. We found that NFL thickness did not change significantly after surgery. This agrees with previous studies, which showed either no change after IOP-lowering interventions<sup>36</sup>, inconsistent fluctuations<sup>37</sup>, or continued thinning<sup>38</sup>.

The ONH structure tells a more complicated story than the NFL. Several studies have documented increased ONH rim and reduced cupping after trabeculectomy<sup>38–40</sup>. We also found reduced cup-to-disc ratio and increased rim area. These changes, again, occurred gradually and lagged IOP reduction, suggesting that the phenomenon may be due to tissue remodeling rather than elastic rebound. The ONH changes were unlikely to be due to regeneration of nerve fibers, since NFL thickness did not increase after intervention. Therefore, the restoration of ONH rim area was likely due to the anterior migration of the scleral attachment of the lamina cribrosa—a reversal of the posterior migration that is known to occur in glaucoma<sup>41</sup>. Thus we do not believe that ONH structural recovery and NFLP perfusion recovery are causally related to each other in a direct way, although both are the sequelae of IOP reduction in glaucomatous eyes.

An exciting implication of our findings is that OCTA parameters could be used as pharmacodynamic biomarkers to assess the response to glaucoma treatments that are not based on lowering the IOP. Unlike ONH

structural parameters, which measures IOP-mediated biomechanical changes and tissue remodeling, NFLP perfusion parameters respond to the metabolic demands of ganglion cells and nerve fibers. Thus if a neuroprotective agent could rescue viable but dysfunctional ganglion cells<sup>42–44</sup>, its effect could theoretically be measured by improvements in NFLP-CD or LPA. The excellent correlation between these OCTA parameters and VF parameters also support this possibility<sup>15,45,46</sup>. There is a great need for more precise objective biomarkers because VF parameters have high measurement variability<sup>47,48</sup> and require large cohorts and many tests over extended follow-up periods to show significant improvement or slowing of progression. Even the memantine study, with over 2000 patients and 48 months of follow-up, fell short of statistical significance in demonstrating the slowing of VF progression<sup>42</sup>. As our study shows, OCTA could demonstrate a highly significant treatment effect with only a small sample followed over a 6-month period, when VF parameters showed only small changes that were far from statistical significance. However, further studies are needed to verify that the short-term improvement in OCTA perfusion parameters could be linked to either long-term VF improvement or slow-down in progression.

Our results also suggest that OCT and OCTA parameters could be useful as predictive biomarkers—peripapillary areas with minimal NFL thinning and moderate NFLP-CD loss were most likely to recover. However, the level of agreement between predicted and actual recovery was only fair. Thus, its utility for individual patients may be limited. But these parameters could still be useful for the selection of patients most likely to respond to certain therapies on a group basis.

While we suggest many possible implications of our results, we realize that our study is limited to a short-term follow-up of a small sample of POAG patients that underwent IOP-lowering surgery. Some postoperative changes may be confounding. Stopping of glaucoma medications postoperatively may influence retinal perfusion, although published results so far only showed that medications have no change or improved capillary density<sup>49,50</sup>. Ocular surface changes may affect the quality of OCTA images, although our signal strength analysis showed that preoperative and postoperative images quality were comparable. Larger and longer studies are needed with more diverse glaucoma types and interventions.

In conclusion, OCTA showed that peripapillary NFLP perfusion gradually improved over 6 months after IOP-lowering surgery in glaucoma patients. The perfusion recovery tended to occur in areas with minimal NFL thinning and moderate perfusion loss. These findings suggest that OCTA parameters may have value in future studies to determine its potential usefulness as pharmacodynamic biomarkers for the recovery of dysfunctional but viable ganglion cells. They might be helpful in clinical trials of novel glaucoma treatments.

## Methods

**Study population.** This prospective cohort study was performed from May 6, 2014 to February 11, 2016 at the Casey Eye Institute, Oregon Health & Science University (OHSU). The research protocols were approved by the Institutional Review Board at OHSU, and carried out in accordance with the tenets of the Declaration of Helsinki. Written informed consent was obtained from each participant.

The participants were part of the “Functional and Structural Optical Coherence Tomography for Glaucoma” study. The participants were enrolled at the Glaucoma Clinic of the Casey Eye Institute by the clinical investigators. All participants had progressive perimetric glaucoma (PG) and were scheduled to undergo trabeculectomy or canaloplasty surgery to lower intraocular pressure (IOP). The inclusion criteria were: (1) an optic disc rim defect (thinning or notching) or NFL defect visible on slit-lamp biomicroscopy; and (2) a consistent glaucomatous pattern, on both qualifying Humphrey SITA 24-2 VFs, meeting at least one of the following criteria: pattern standard deviation (PSD) outside normal limits ( $P < 0.05$ ) or glaucoma hemifield test outside normal limits.

The exclusion criteria were: (1) best-corrected visual acuity (BCVA) worse than 20/40; (2) age  $< 30$  or  $> 80$  years; (3) refractive error of  $> +3.00$  D or  $< -7.00$  D; (4) previous intraocular surgery except for an uncomplicated cataract extraction with posterior chamber intraocular lens implantation; (5) any diseases that may cause VF loss or optic disc abnormalities; or (6) inability to perform reliably on automated VF testing. One eye from each participant was scanned and analyzed.

All ocular antihypertensive medications were continued up to the time of surgery. Eyes with signs of hypotony, maculopathy, or disc edema after surgery were excluded from analysis.

**Visual field testing.** VF tests were performed with the Humphrey Field Analyzer II (Carl Zeiss, Inc.) set for the 24-2 threshold test, size III white stimulus, using the SITA standard algorithm. VF testing was done within 1 month prior to the surgery and 3 and 6 months after the surgery.

**Optical coherence tomography equipment.** A 70-kHz, 840-nm wavelength spectral-domain OCT system (Avanti, Optovue Inc.) with the AngioVue OCTA software (Version 2016.2.0.35) was used.

**Image acquisition and processing.** Pharmacologic pupil dilation was used for OCTA scanning to optimize image quality. The peripapillary retinal region was scanned using a  $4.5 \times 4.5$ -mm volumetric angiography scan centered on the optic disc. Each volume was comprised of 304 line-scan locations<sup>20,21</sup>. Two sets of scans were performed within one visit. The OCT angiogram with higher signal strength index (SSI) was used in the following analysis. The OCTA scan was done within 1 month prior to the surgery for the glaucoma patients and 6 weeks, 3 months and 6 months after the surgery.

The merged volumetric angiograms were then exported for custom processing using the Center for Ophthalmic Optics & Lasers-Angiography Reading Toolkit (COOL-ART) software<sup>51</sup>. The OCTA scans contained both volumetric flow (decorrelation) data as well as structural (reflectance) data. Segmentation of the retinal layers was performed by automated MATLAB programs that operate on the structural OCT data. Further manual correction of the segmentation was conducted by certified graders, if required. An en face angiogram of retinal

nerve fiber layer plexus (NFLP) was obtained by maximum flow (decorrelation value) projection. The NFLP slab was bounded by the inner limiting membrane and the outer edge of the nerve fiber layer.

**OCT angiography measurements.** In order to achieve good alignment between preoperative and postoperative OCTA images, the analytic area was cropped to 4 × 4-mm from 4.5 × 4.5-mm OCTA scan. The analytic area was manually centered on the optic disc based on the en face reflectance image excluding the central 2 mm diameter circle. The NFLP capillary density (NFLP-CD) was defined as the percentage area occupied by capillaries. Arterioles and venules (larger vessels) were automatically identified by thresholding the en face mean projection of OCT reflectance signal within the retinal slab. After these larger vessels were excluded, the remaining angiogram was used to compute capillary density. A reflectance-adjustment algorithm was used to correct the artifactually lower flow signal in regions of reduced reflectance (e.g. due to media opacity or pupil vignetting)<sup>52</sup>. Previous clinical validation has shown this algorithm was able to remove the dependence of retinal OCTA measurements on the signal strength index and reduce population variation<sup>45,52</sup>. A scan was considered to be grossly decentered if the 4 × 4-mm analytic area was cropped by more than 5%. Grossly decentered scans were excluded.

The *en face* OCTA of the NFLP and the 24-2 VF total deviation map were divided into 8 corresponding sectors according to an extended Garway-Heath scheme (Fig. 1). The original Garway-Heath scheme divided the disc rim into 6 sectors<sup>53,54</sup>. We added horizontal dividing lines to the original nasal and temporal sectors to increase the total number of sectors to 8<sup>29</sup>. The sector boundaries were extended outward along nerve fiber trajectories obtained from structural OCT nerve fiber flux analysis<sup>55</sup>. The sectoral NFLP-CD and NFL thickness were converted to percent loss, ranging from 0 to 100%, according to the equation:

$$\% \text{ Loss} = 100 \times (\text{N} - \text{value})/\text{N},$$

where N is the average value in age-matched normal subjects in the FS-OCT study<sup>17</sup>.

Another OCTA outcome measure was the low-perfusion area (LPA). The low-perfusion map and LPA assessed the location and severity of focal glaucoma damage with good agreement with VF<sup>29</sup>. Low perfusion was defined as CD below the 0.5 percentile normative threshold in a contiguous area of at least 0.053 mm<sup>2</sup> (98.5 normative cutoff). The low-perfusion map displayed normal perfusion in green and abnormally low perfusion in red (Fig. 1). The LPA in each eye was defined by the cumulative area of pixels that met the low perfusion criteria.

Image quality was assessed for all OCTA scans. Poor quality scans with signal strength index (SSI) below 50, or registered image sets with residual motion artifacts (discontinuous vessel pattern) were excluded from analysis.

**Structural OCT measurements.** All the structural OCT parameters were measured from OCTA scans. The retinal NFL thickness was measured along 3.45-mm diameter annulus of 0.1-mm width centered on the optic disc.

The optic nerve head (ONH) rim area, cup volume and cup/disc area ratio were calculated using Angio-Analytics (version 2018.1.0.22, Optovue Inc, Fremont, CA). The optic disc boundary was defined by the Bruch's membrane opening. The Bruch's membrane opening plane was used as the reference plane to separate the neuroretinal rim from the cup.

**Statistical analysis.** The Friedman test, which is a nonparametric alternative for repeated-measures analysis of variance, was used to analyze the differences across multiple visits. Wilcoxon signed-rank test was used to compare between two visits. Spearman correlation was used to determine the relationships between the changes of OCT/OCTA parameters with the changes of IOP and VF parameters. In order to investigate the correlations between preoperative OCT/OCTA parameters and postoperative perfusion recovery potential, univariate and multivariate regression analyses were used. A linear mixed-effects model was used to account for within-subject correlation in sectoral analysis; the subject identity was treated as a random effect. All statistical analyses were performed with SPSS 20.0 (SPSS Inc., Chicago, IL) and MedCalc 10.1.3.0 (MedCalc Software, Ostend, Belgium, [www.medcalc.be](http://www.medcalc.be)). The statistical significance was assumed at P < 0.05.

Received: 16 February 2021; Accepted: 6 August 2021

Published online: 26 August 2021

## References

1. Tham, Y. C. *et al.* Global prevalence of glaucoma and projections of glaucoma burden through 2040: A systematic review and meta-analysis. *Ophthalmology* **121**, 2081–2090 (2014).
2. Eye Diseases Prevalence Research Group. Prevalence of open-angle glaucoma among adults in the united states. *Arch. Ophthalmol.* **122**, 532–538 (2004).
3. Musch, D. C. *et al.* Visual field improvement in the collaborative initial glaucoma treatment study. *Am. J. Ophthalmol.* **158**, 96–104 (2014).
4. Caprioli, J. *et al.* Trabeculectomy can improve long-term visual function in glaucoma. *Ophthalmology* **123**, 117–128 (2016).
5. Baril, C. *et al.* Rates of glaucomatous visual field change after trabeculectomy. *Br. J. Ophthalmol.* **101**, 874–878 (2017).
6. Tavares, I. M. *et al.* No changes in anatomical and functional glaucoma evaluation after trabeculectomy. *Graefes Arch. Clin. Exp. Ophthalmol.* **244**, 545–550 (2006).
7. Nouri-Mahdavi, K. *et al.* Predictive factors for glaucomatous visual field progression in the advanced glaucoma intervention study. *Ophthalmology* **111**, 1627–1635 (2004).
8. Heijl, A. *et al.* Reduction of intraocular pressure and glaucoma progression: Results from the early manifest glaucoma trial. *Arch. Ophthalmol.* **120**, 1268–1279 (2002).

9. Anton, A. *et al.* Glaucoma progression detection: Agreement, sensitivity, and specificity of expert visual field evaluation, event analysis, and trend analysis. *Eur. J. Ophthalmol.* **23**, 187–195 (2013).
10. Artes, P. H. *et al.* Properties of the statpac visual field index. *Investig. Ophthalmol. Vis. Sci.* **52**, 4030–4038 (2011).
11. Lee, J. M. *et al.* Performance of the visual field index in glaucoma patients with moderately advanced visual field loss. *Am. J. Ophthalmol.* **157**, 39–43 (2014).
12. Wu, Z., Saunders, L. J., Daga, F. B., Diniz-Filho, A. & Medeiros, F. A. Frequency of testing to detect visual field progression derived using a longitudinal cohort of glaucoma patients. *Ophthalmology* **124**, 786–792 (2017).
13. Moghimi, S. *et al.* Macular and optic nerve head vessel density and progressive retinal nerve fiber layer loss in glaucoma. *Ophthalmology* **125**, 1720–1728 (2018).
14. Yarmohammadi, A. *et al.* Peripapillary and macular vessel density in patients with primary open-angle glaucoma and unilateral visual field loss. *Ophthalmology* **125**, 578–587 (2018).
15. Liu, L. *et al.* Projection-resolved optical coherence tomography angiography of the peripapillary retina in glaucoma. *Am. J. Ophthalmol.* **207**, 99–109 (2019).
16. Yarmohammadi, A. *et al.* Optical coherence tomography angiography vessel density in healthy, glaucoma suspect, and glaucoma eyes. *Investig. Ophthalmol. Vis. Sci.* **57**, 451–459 (2016).
17. Liu, L. *et al.* Sectorwise visual field simulation using optical coherence tomographic angiography nerve fiber layer plexus measurements in glaucoma. *Am. J. Ophthalmol.* **212**, 57–68 (2020).
18. Bowd, C. *et al.* Gradient-boosting classifiers combining vessel density and tissue thickness measurements for classifying early to moderate glaucoma. *Am. J. Ophthalmol.* **217**, 131–139 (2020).
19. Yu, J. J. *et al.* Signal strength reduction effects in OCT angiography. *Ophthalmol. Retina* **3**, 835–842 (2019).
20. Kamalipour, A. *et al.* OCT angiography artifacts in glaucoma. *Ophthalmology*. <https://doi.org/10.1016/j.ophtha.2021.03.036> (2021).
21. Rao, H. L. *et al.* A comparison of the diagnostic ability of vessel density and structural measurements of optical coherence tomography in primary open angle glaucoma. *PLoS ONE* **12**, e0173930 (2017).
22. Chen, C.-L. *et al.* Peripapillary retinal nerve fiber layer vascular microcirculation in glaucoma using optical coherence tomography-based microangiography. *Investig. Ophthalmol. Vis. Sci.* **57**, 475–485 (2016).
23. Kim, J. A., Kim, T. W., Lee, E. J., Girard, M. J. A. & Mari, J. M. Microvascular changes in peripapillary and optic nerve head tissues after trabeculectomy in primary open-angle glaucoma. *Investig. Ophthalmol. Vis. Sci.* **59**, 4614–4621 (2018).
24. In, J. H., Lee, S. Y., Cho, S. H. & Hong, Y. J. Peripapillary vessel density reversal after trabeculectomy in glaucoma. *J. Ophthalmol.* **2018**, 8909714 (2018).
25. Shin, J. W. *et al.* Peripapillary microvascular improvement and lamina cribrosa depth reduction after trabeculectomy in primary open-angle glaucoma. *Investig. Ophthalmol. Vis. Sci.* **58**, 5993–5999 (2017).
26. Hollo, G. Influence of large intraocular pressure reduction on peripapillary OCT vessel density in ocular hypertensive and glaucoma eyes. *J. Glaucoma* **26**, e7–e10 (2017).
27. Zeboulon, P. *et al.* Effect of surgical intraocular pressure lowering on peripapillary and macular vessel density in glaucoma patients: An optical coherence tomography angiography study. *J. Glaucoma* **26**, 466–472 (2017).
28. Ch'ng, T. W. *et al.* Effect of surgical intraocular pressure lowering on retinal structures—Nerve fibre layer, foveal avascular zone, peripapillary and macular vessel density: 1 year results. *Eye (Lond.)* **34**, 562–571 (2020).
29. Chen, A. *et al.* Measuring glaucomatous focal perfusion loss in the peripapillary retina using OCT angiography. *Ophthalmology* **127**, 484 (2020).
30. Jia, Y. *et al.* Wide-field OCT angiography investigation of the relationship between radial peripapillary capillary plexus density and nerve fiber layer thickness. *Invest. Ophthalmol. Vis. Sci.* **58**, 5188–5194 (2017).
31. Hodapp, E. P. R. I. & Anderson, D. R. *Clinical Decisions in Glaucoma* 52–61 (The CV Mosby Co, 1993).
32. Lommatzsch, C., Rothaus, K., Koch, J. M., Heinz, C. & Grisanti, S. Retinal perfusion 6 months after trabeculectomy as measured by optical coherence tomography angiography. *Int. Ophthalmol.* **39**, 2583–2594 (2019).
33. Fry, L. E. *et al.* The coma in glaucoma: Retinal ganglion cell dysfunction and recovery. *Prog. Retin. Eye Res.* **65**, 77–92 (2018).
34. Waisbourd, M. *et al.* Reversible structural and functional changes after intraocular pressure reduction in patients with glaucoma. *Graefes Arch. Clin. Exp. Ophthalmol.* **254**, 1159–1166 (2016).
35. Wright, T. M., Goharian, I., Gardiner, S. K., Sehi, M. & Greenfield, D. S. Short-term enhancement of visual field sensitivity in glaucomatous eyes following surgical intraocular pressure reduction. *Am. J. Ophthalmol.* **159**, 378–385 (2015).
36. Chang, P. T. *et al.* Effect of lowering intraocular pressure on optical coherence tomography measurement of peripapillary retinal nerve fiber layer thickness. *Ophthalmology* **114**, 2252–2258 (2007).
37. Raghun, N., Pandav, S. S., Kaushik, S., Ichhpujani, P. & Gupta, A. Effect of trabeculectomy on RNFL thickness and optic disc parameters using optical coherence tomography. *Eye (Lond.)* **26**, 1131–1137 (2012).
38. Lee, E. J. & Kim, T.-W. Lamina cribrosa reversal after trabeculectomy and the rate of progressive retinal nerve fiber layer thinning. *Ophthalmology* **122**, 2234–2242 (2015).
39. Sanchez, F. G. *et al.* Effect of trabeculectomy on OCT measurements of the optic nerve head neuroretinal rim tissue. *Ophthalmol. Glaucoma* **3**, 32–39 (2020).
40. Kadziauskiene, A. *et al.* Long-term shape, curvature, and depth changes of the lamina cribrosa after trabeculectomy. *Ophthalmology* **125**, 1729–1740 (2018).
41. Yang, H. *et al.* Posterior (outward) migration of the lamina cribrosa and early cupping in monkey experimental glaucoma. *Investig. Ophthalmol. Vis. Sci.* **52**, 7109–7121 (2011).
42. Weinreb, R. N. *et al.* Oral memantine for the treatment of glaucoma: Design and results of 2 randomized, placebo-controlled, phase 3 studies. *Ophthalmology* **125**, 1874–1885 (2018).
43. WoldeMussie, E., Ruiz, G., Wijono, M. & Wheeler, L. A. Neuroprotection of retinal ganglion cells by brimonidine in rats with laser-induced chronic ocular hypertension. *Investig. Ophthalmol. Vis. Sci.* **42**, 2849–2855 (2001).
44. Saylor, M., McLoon, L. K., Harrison, A. R. & Lee, M. S. Experimental and clinical evidence for brimonidine as an optic nerve and retinal neuroprotective agent: An evidence-based review. *Arch. Ophthalmol.* **127**, 402–406 (2009).
45. Takusagawa, H. L. *et al.* Projection-resolved optical coherence tomography angiography of macular retinal circulation in glaucoma. *Ophthalmology* **124**, 1589–1599 (2017).
46. Yarmohammadi, A. *et al.* Relationship between optical coherence tomography angiography vessel density and severity of visual field loss in glaucoma. *Ophthalmology* **123**, 2498–2508 (2016).
47. Birt, C. M. *et al.* Analysis of reliability indices from Humphrey visual field tests in an urban glaucoma population. *Ophthalmology* **104**, 1126–1130 (1997).
48. Gordon, M. O. *et al.* The ocular hypertension treatment study: Baseline factors that predict the onset of primary open-angle glaucoma. *Arch. Ophthalmol.* **120**, 714–720 (2002).
49. Chihara, E., Dimitrova, G. & Chihara, T. Increase in the OCT angiographic peripapillary vessel density by ROCK inhibitor ripasudil instillation: A comparison with brimonidine. *Graefes Arch. Clin. Exp. Ophthalmol.* **256**, 1257–1264 (2018).
50. Liu, C. *et al.* The effect of medical lowering of intraocular pressure on peripapillary and macular blood flow as measured by optical coherence tomography angiography in treatment-naïve eyes. *J. Glaucoma* **30**, 465–472 (2021).
51. Zhang, M. *et al.* Advanced image processing for optical coherence tomographic angiography of macular diseases. *Biomed. Opt. Express* **6**, 4661–4675 (2015).

52. Gao, S. S. *et al.* Compensation for reflectance variation in vessel density quantification by optical coherence tomography angiography. *Investig. Ophthalmol. Vis. Sci.* **57**, 4485–4492 (2016).
53. Le, P. V. *et al.* Regional correlation among ganglion cell complex, nerve fiber layer, and visual field loss in glaucoma. *Investig. Ophthalmol. Vis. Sci.* **54**, 4287–4295 (2013).
54. Garway-Heath, D. F., Poinoosawmy, D., Fitzke, F. W. & Hitchings, R. A. Mapping the visual field to the optic disc in normal tension glaucoma eyes. *Ophthalmology* **107**, 1809–1815 (2000).
55. Tan, O., Liu, L., Liu, L. & Huang, D. Nerve fiber flux analysis using wide-field swept-source optical coherence tomography. *Transl. Vis. Sci. Technol.* **7**, 16 (2018).

### Author contributions

Conception or design of the work (all authors). Data Collection (T.H., E.B. and J.C.). Data analysis and interpretation (all authors). Creation of new software used in this study (W.J., Y.J. and T.O.) Drafting the article (L.L., T.H., G.M., A.B. and D.H.). Final approval (all authors).

### Funding

NIH Grants R01 EY023285, R01 EY010145, R21 EY027007, P30 EY010572, and unrestricted departmental funding from Research to Prevent Blindness (New York, NY).

### Competing interests

OHSU, Yali Jia, Ou Tan and David Huang have financial interest in Optovue, Inc., a company that may have a commercial interest in the results of this research and technology. These potential conflicts of interest have been reviewed and are managed by OHSU. The other authors do not report any potential financial conflicts of interest.

### Additional information

**Supplementary Information** The online version contains supplementary material available at <https://doi.org/10.1038/s41598-021-96225-7>.

**Correspondence** and requests for materials should be addressed to D.H.

**Reprints and permissions information** is available at [www.nature.com/reprints](http://www.nature.com/reprints).

**Publisher's note** Springer Nature remains neutral with regard to jurisdictional claims in published maps and institutional affiliations.



**Open Access** This article is licensed under a Creative Commons Attribution 4.0 International License, which permits use, sharing, adaptation, distribution and reproduction in any medium or format, as long as you give appropriate credit to the original author(s) and the source, provide a link to the Creative Commons licence, and indicate if changes were made. The images or other third party material in this article are included in the article's Creative Commons licence, unless indicated otherwise in a credit line to the material. If material is not included in the article's Creative Commons licence and your intended use is not permitted by statutory regulation or exceeds the permitted use, you will need to obtain permission directly from the copyright holder. To view a copy of this licence, visit <http://creativecommons.org/licenses/by/4.0/>.

© The Author(s) 2021